agronomy

MDPI

Article

Evaluation of Image-Based Phenotyping Methods for Measuring Water Yam (*Dioscorea alata* L.) Growth and Nitrogen Nutritional Status under Greenhouse and Field Conditions

Emmanuel Frossard [1,*,†], Frank Liebisch [2,3,†], Valérie Kouamé Hgaza [4,5], Delwendé Innocent Kiba [1,6], Norbert Kirchgessner [2], Laurin Müller [1,2], Patrick Müller [1,2], Nestor Pouya [7], Cecil Ringger [1,2,3] and Achim Walter [2]

1 Group of Plant Nutrition, Institute of Agricultural Sciences, ETH Zurich, 8315 Zurich, Switzerland; delwende.kiba@usys.ethz.ch (D.I.K.); muellaur@gmail.com (L.M.); mupatric@student.ethz.ch (P.M.); cecil.ringger@agroscope.admin.ch (C.R.)
2 Group of Crop Science, Institute of Agricultural Sciences, ETH Zurich, 8092 Zurich, Switzerland; frank.liebisch@agroscope.admin.ch (F.L.); norbert.kirchgessner@usys.ethz.ch (N.K.); achim.walter@usys.ethz.ch (A.W.)
3 Agroecology and Environment, Agroscope, 8046 Zurich, Switzerland
4 Centre Suisse de Recherches Scientifiques, 01 BP 1303 Abidjan, Cote D'Ivoire; hgaza.kouame@csrs.ci
5 Département d'Agrophysiologie des Plantes, Université Peleforo Gon Coulibaly, BP 1328 Korhogo, Cote D'Ivoire
6 Institut de l'Environnement et Recherches Agricoles, 04 BP 8645 Ouagadougou, Burkina Faso
7 Laboratory of Plant Physiology, Université Félix Houphouët Boigny, 01 BP V34 Abidjan, Cote D'Ivoire; nestaledja@gmail.com
* Correspondence: emmanuel.frossard@usys.ethz.ch; Tel.: +41-52-354-91-40
† Both first authors (E.F. and F.L.) have contributed in the same manner to this paper.

Abstract: New management practices must be developed to improve yam productivity. By allowing non-destructive analyses of important plant traits, image-based phenotyping techniques could help developing such practices. Our objective was to determine the potential of image-based phenotyping methods to assess traits relevant for tuber yield formation in yam grown in the glasshouse and in the field. We took plant and leaf pictures with consumer cameras. We used the numbers of image pixels to derive the shoot biomass and the total leaf surface and calculated the 'triangular greenness index' (TGI) which is an indicator of the leaf chlorophyll content. Under glasshouse conditions, the number of pixels obtained from nadir view (view from the top) was positively correlated to shoot biomass, and total leaf surface, while the TGI was negatively correlated to the SPAD values and nitrogen (N) content of diagnostic leaves. Pictures taken from nadir view in the field showed an increase in soil surface cover and a decrease in TGI with time. TGI was negatively correlated to SPAD values measured on diagnostic leaves but was not correlated to leaf N content. In conclusion, these phenotyping techniques deliver relevant results but need to be further developed and validated for application in yam.

Keywords: leaf surface; soil surface cover; growth rate; nitrogen leaf content; SPAD; triangular greenness index (TGI)

check for updates

Citation: Frossard, E.; Liebisch, F.; Hgaza, V.K.; Kiba, D.I.; Kirchgessner, N.; Müller, L.; Müller, P.; Pouya, N.; Ringger, C.; Walter, A. Evaluation of Image-Based Phenotyping Methods for Measuring Water Yam (*Dioscorea alata* L.) Growth and Nitrogen Nutritional Status under Greenhouse and Field Conditions. *Agronomy* **2021**, *11*, 249. https://doi.org/10.3390/agronomy11020249

Academic Editor: Andreas Stahl
Received: 12 December 2020
Accepted: 26 January 2021
Published: 29 January 2021

Publisher's Note: MDPI stays neutral with regard to jurisdictional claims in published maps and institutional affiliations.

1. Introduction

Yam (*Dioscorea* spp.) tuber is a staple food for millions of people in tropical areas [1]. West Africa produces more than 90% of the world tuber production over 8.5 million of hectares [1,2]. The average tuber production in West Africa remains however low (around 10 t fresh tuber ha^{-1}) compared to 50 t fresh tuber ha^{-1} that can be produced under well-managed conditions [2,3]. As population is still growing at a fast pace in West Africa, yam tuber demand will probably further increase. Therefore, it is urgent to develop cropping practices to sustainably increase the productivity of this under-researched crop [4].

Important traits for tuber yield formation are: (i) emergence rate as the first emerged plants contribute most to the final tuber yield measured at field level [5,6]; (ii) foliage development as maximum leaf area index is correlated to final tuber yield [7] due to improved light interception, and lower weed infestation and soil erosion [3]; and (iii) the N nutritional status, because N leaf status is one of the main factors driving leaf formation and growth [7]. Conducting field experiments to study these factors with destructive sampling requires large fields, a lot of time and labor. Indeed, in such experiments yams are planted at a density of one plant per m^2, the leaf area index can reach values of up to eight, this plant can reach a height of several meters if it finds a climbing support and the growth period may last nine months. The destructive sampling used to measure plant biomass, leaf surface and N uptake with time further increases the variability of results due to the variability that exists between individual plants which decreases our ability to statistically detect differences associated with specific treatments. Following single plants during the growing season with non-destructive methods would therefore be useful to study more precisely the impacts of specific treatments on yam growth under field conditions.

Image-based phenotyping is widely used to analyze plant traits such as germination rate, leaf surface, and growth rate of cereals and legumes [8–11]. More recently image-based phenotyping was successfully adapted for root and tuber crops such as sugar beet and potato [12–15]. Serial imaging, by Red Green Blue (RGB) cameras (consumer cameras) coupled with appropriate segmentation techniques and image analysis delivers information on plant growth, and soil cover [16]. In addition, leaf spectral indices derived from the visible and near-infrared ranges of the light spectrum, such as the triangular greenness index (TGI) provide information on the leaf chlorophyll content [10]. As a large fraction of leaf N is located in photosynthesis related proteins [17], TGI could potentially also inform on the N nutrition status of crops. Such imaging approaches could therefore be useful for studying yam growth under field conditions.

There is little information on the use of image-based phenotyping to assess the growth, biomass and N nutritional status of tropical root and tuber crops. Phenotyping of these crops is challenging as they have often a more complex morphology and growth habitus than temperate crops such as wheat, maize and soybean. Iseki and Matsumoto [18] developed a model for shoot dry matter production of a white guinea yam (*D. rotundata*) cultivar grown over several months using a sensor measuring the green area of the plant and the plant height. The model underestimated dry plant weight when it was higher than 150 g and the predicted biomass showed a high variability. This model did not predict leaf surface nor the N plant content. Other authors have used image analysis to assess the prevalence of diseases on yam and cassava leaves [19–21].

The objective of this paper was to determine the potential of image-based phenotyping methods to assess yam traits that are relevant for tuber yield formation. The traits considered in this paper were leaf surface, shoot biomass, and the plant N status measured until six to nine weeks after emergence. This work focused on water yam (*D. alata*) because it is grown all over the tropics. Since published information on yam phenotyping methodology is scarce, we first analyzed the feasibility of detecting the above-mentioned traits under greenhouse conditions by comparing data derived from the phenotyping approaches to those measured with classical methods and subsequently we tested the imaging approach in a field experiment conducted in the center of Côte d'Ivoire.

2. Materials and Methods

2.1. Greenhouse Experiments

We conducted two greenhouse experiments at the ETH Zurich plant research station in Eschikon (47°26′ N 8°40′ E, 520 m above sea level). The first was conducted from July to October 2015 by Ringger [22], and the second from December 2016 to March 2017 by Müller [23]. Since both experiments delivered similar results, although they were based on slightly different designs, we only present the results of the 2nd experiment in the main

part of this paper. The materials and methods and the main results of the 1st experiment are shown in the Supplementary Materials.

2.1.1. Plant Material, Growth Conditions and Experimental Design

We grew the water yam cultivar "raja ala" from Sri Lanka, which was imported to Zurich by SK Trading GmbH, Zurich, Switzerland. We used the minisett technique to install the experiment [24]. Head parts of healthy-looking tubers were cut into minisetts of about 70 g fresh weight. Each minisett was dipped for ten minutes in a fungicide solution of 2.5 g MALVIN® WG per L water (active substance captan) before planting. One minisett was planted per pot at 8 to 10 cm depth, with the peel (periderm) facing downwards.

A total of 60 minisetts were planted into plastic pots (2.9 L volume, 16 cm diameter, 18 cm height), filled with 1.0 kg substrate (dry weight). The substrate, a coarse grained attapulgite clay granulate (Oil-Dri US-Special, Oilbinder Type III R, Damolin Mettmann GmbH, Oberhausen, Germany) has low total N content (0.3 g kg^{-1} substrate), good structure, and high water holding capacity. Four wooden sticks were installed on the edge of each pot and painted in blue for vine training and climbing. Plants were irrigated with tap water every second to third day. Temperature ranged between 24 °C and 27 °C during the day and between 20 °C and 22 °C during the night. Relative atmospheric humidity was 60% during the day and 65% during the night. Metal-halid lamps (Type PF400S, Hugentobler Spezialleuchten AG, Weinfelden Switzerland) were adjusted 1.80 m above the greenhouse table, to ensure a photoperiod of 12 h d^{-1} at 30 kLux.

As yam tuber sprouting is variable [5], we decided to arrange the pot experiment in three blocks based on the emergence date of the plants. The 20 plants that emerged first formed block one, the following plants that emerged 21st–40th built block two and the last 20 plants made block three. All plants of block one and two emerged within five days each. In block three, 19 out of 20 plants emerged within eight days while the last one emerged ten days after the first emerged plant of block three. The median of all plants per block was selected as emergence date per block. All plants were arranged randomly within each block.

Each block included four N levels: 0, 101, 202 and 342 mg N pot^{-1} (equivalent to 0, 50, 100 and 170 kg N ha^{-1}) which were replicated five times each. Nitrogen was applied in form of calcium nitrate ($Ca(NO_3)_2$). The application of the 50 and 100 kg N ha^{-1} treatment was made two weeks after the corresponding emergence date per block. The 170 kg N ha^{-1} treatment was split into two doses of each 85 kg N ha^{-1} applied 14 and 28 days after emergence. Additionally, each plant received sufficient phosphorus (KH_2PO_4), potassium (K_2SO_4), zinc ($ZnSO_4$) and iron (Fe-Sequestrene) added in a nutrient solution two weeks after emergence. None of the nutrient deficiency symptoms described by O'Sullivan and Jenner [25] were observed during the experiment. Plants did not show any visible signs of diseases or pest attacks during growth.

2.1.2. Sampling and Measurements

We describe here the destructive and non-destructive samplings. The imaging techniques are presented in Section 2.3.

Destructive Sampling for Biomass Production, Total Leaf Area and Leaf N Content

Destructive sampling took place three, six and nine weeks after emergence one day after plant imaging. Block one was harvested after 61 days, block two after 40 days and block three after 20 days. For destructive sampling, all plants of the corresponding block were cut at the level of soil surface. After petioles and leaves were detached from the vines, total vine length was measured. Total fresh shoot biomass (vine, petiole, and leaves) was weighed and dried at 55 °C for at least one week to obtain the total shoot dry weight. Before drying, total leaf area per plant was measured as follow. All leaves of a given plant were spread on a blue background, then nadir images were taken with the indoor imaging station described in Section 2.3.1 and the images were processed using the methodology described

in Section 2.3.3. We determined the N concentrations of the 1st and 7th fully developed leaves counted from the apex of each vine at each harvest. Dried leaves were powdered with a ball mill (Mixer Mill MM200, Retsch GmbH, Haan, Germany) and analyzed using a Flash EA 1112 NC analyzer (Thermo Fisher Scientific, Waltham, MA, USA).

Non-Destructive Sampling for Leaf Number and SPAD Values Analysis

The total number of fully developed leaves was counted weekly, a day before images were taken. Every week the most recently counted leaf was marked with a string. Since leaves of water yam can have an alternate and an opposite arrangement on the vine [25] we counted each node as one leaf regardless if leaves had developed in opposite or alternate order. A SPAD meter (SPAD-502, Minolta Corporation, Ramsey, NJ, USA) was used to estimate the chlorophyll content which is often positively related to the leaf N content [26–28]. The SPAD meter measures light absorption by the leave at 650 nm, which is the wavelength at which chlorophylls a and b absorb light and at 950 nm, which is a wavelength that is theoretically not absorbed by the chloroplast, and it calculates a SPAD value [27]. High amount of chlorophyll in a leaf leads to high absorption in the red spectral range and therefore to an intensive, green coloration of the leaf. In this study the SPAD value was measured on the 7th leaf starting from the apex as the leaf in the first position was generally too small for these measures. Three SPAD measures were taken per leaf and averaged. Leaf properties are variable in yam. We considered the 7th fully developed leaf from the vine apex as a diagnostic leaf because the SPAD, N content, and leaf area reach a stable value from the 6th leaf on, while leaf conductance is at its maximum between leaf 5 and 10 [29].

2.2. Field Experiment

The field experiment was conducted by Müller [30]. We present thereafter the site, the experimental design, the installation of the field experiment and the methods used. The imaging techniques are presented in Section 2.3.

2.2.1. Site Description

In May 2018, a field experiment was installed in Tieningboué, Côte d'Ivoire (8°11′ N 5°43′ W, 317 m above sea level) on an acric plinthic Ferralsol [31,32]. The upper horizon of this soil (0–22 cm) contained 140 g clay kg^{-1} soil, 6.7 g C kg^{-1} soil, 0.47 g N kg^{-1} soil and had a pH in water of 5.1 [32]. The site is located in the Center of Côte d'Ivoire, in the Béré region, department of Mankono. The area of Tieningboué is characterized by a tropical climate with a dry season (October to February) and a rainy season (March to September). The climatic data of the season 2018 were recorded with a Campbell Scientific CR1000 weather station and are shown in the Supplementary Materials (Figure S5).

2.2.2. Experimental Design

We tested the use of image-based phenotyping in a single block of a large field experiment assessing the impact of crop rotation and fertilization on yam growth. The trial was started in 2016 and was in its 3rd year. The four studied rotations were water yam—rice—water yam (R1), water yam—groundnut—water yam (R2), water yam intercropped with maize—rice—water yam (R3), and water yam—white guinea yam—water yam (R4). There were four fertilization treatments T0, T1, T2 and T3. The treatment T0 (no fertilization) received no nutrient input. The treatment T1 (fully mineral) received NPK for a target yield of 25 t fresh tuber ha^{-1} (56 kg N ha^{-1}, 8 kg P ha^{-1}, 80 kg K ha^{-1}) in the form of mineral fertilizers (urea, super triple phosphate, K_2SO_4). The treatment T2 (organo-mineral) received half of the NPK added as mineral fertilizers plus poultry manure added at the rate of 3.9 t manure fresh weight ha^{-1} bringing 76, 41 and 50 kg N, P, and K (total elements) ha^{-1}. The treatment T3 (fully organic) received only poultry manure at the rate of 7.8 t ha^{-1}, bringing 152, 82 and 100 kg N, P, and K ha^{-1}. The mineral fertilizers (NPK) were broadcasted at equal doses on 10 July 2018 and on 29 August 2018 for T1. In T2,

manure was added on 22 May 2018 just before mound preparation, while mineral NPK fertilizers were broadcasted on 29 August 2018. Finally, in T3 the manure was also added on 22 May 2018 before preparing the mound.

The image-based phenotyping was tested on each one of the following combinations (R1T0, R1T1, R1T2, R1T3, R2T0, R2T1, R2T2, R2T3, R3T0, R3T1, R3T2, R3T3, R4T0, R4T1, R4T2, R4T3) on two plants per plot making a total of 16 plots or 32 plants. We had no replicated treatment in this imaging experiment. With this design we wanted to trigger a large variation in early growth traits such as soil surface cover by yam shoots, and leaf N content.

2.2.3. Installation of the Field Experiment

We used the late maturing water yam cultivar C18 bred by IITA [33]. Healthy tubers were selected and cut in setts of 200 g fresh weight. These setts were dipped in a suspension containing wood ash (15 g L^{-1}) and the fungicide mancozeb (12 g L^{-1}) for 10 min and dried for 24 h in the shade. Fifty cm high mounds were prepared at a density of one mound per square meter. The setts were inserted within the center of mound at 20 cm depth. A single plot (4 m by 5 m) was composed of six central plants installed in two rows of three plants surrounded by 14 border plants. Two of the central plants were used for imaging (see Section 2.3). Head parts of tuber setts were used as planting material for the six central plants to ensure a homogeneous germination, while other parts of tuber setts were used for the border plants. Each plot was separated from the next one by a distance of 1.5 m. Planting was done on 29 May 2018, 80% of the central plants had germinated on 28 June 2018, tuber initiation was reached around 20 August 2018, and tubers were harvested when plants were senescent on 12 December 2018. Manual weeding was organized both to limit competition between yams and other plants and to avoid problems for later image analysis caused by non-yam vegetation. Plants did not show visible symptoms of diseases or signs of pest attacks during their growth.

2.2.4. Sampling and Measurements

Soil surface cover by leaves and plant TGI were measured from 5 July 2018 to 10 August 2018 by imaging (see Section 2.3). Leaves located between the 6th and 8th positions from the apex of the main vine were marked and used to measure the SPAD values as described above. Five readings were taken and averaged per leaf. Leaves were sampled after SPAD measurement, dried in an oven at 50 °C for two days and powdered with a ball mill (Mixer Mill MM200, Retsch GmbH, Haan, Germany) and analyzed for N as already described. SPAD values were measured on 14 July, 8 and 10 August 2018, while N leaf content was measured only on 8 and 10 August 2018. SPAD and leaf N contents were measured on the plants that were analyzed by imaging.

Tuber yields could not be measured on our 16 plots, but they were measured on the four neighboring blocks located 20 m away from our plots (same soil and climate), studying the effects of the same rotations and fertilizations treatments on the C18 cultivar.

2.3. Imaging Devices, Acquisition, and Analysis

2.3.1. Imaging in the Greenhouse Experiment

Images of entire plants or spread out leaves were taken in the greenhouse studies with a custom-made indoor imaging station consisting of a blue background and two cameras for nadir view and side view, respectively (Figure 1). Blue plastic plates (Kömatex, Switzerland) were horizontally and vertically installed forming the background, respectively allowing convenient separation of plant and background in the image. Each pot was placed in a hole of the horizontal plate excluding it from side view images. For the imaging from nadir view, the visible soil and pot surface was covered with blue-plate pieces, so the plant was in front of a completely blue background. Two commercially available 18 Megapixel RGB cameras (Canon EOS 600D) were installed above and beside the imaging station on a steel

framework (Figure 1a) with a non-modified 22.3 × 14.9 mm sensor and a corresponding lens (Canon EF 20 mm f/2.8 USM).

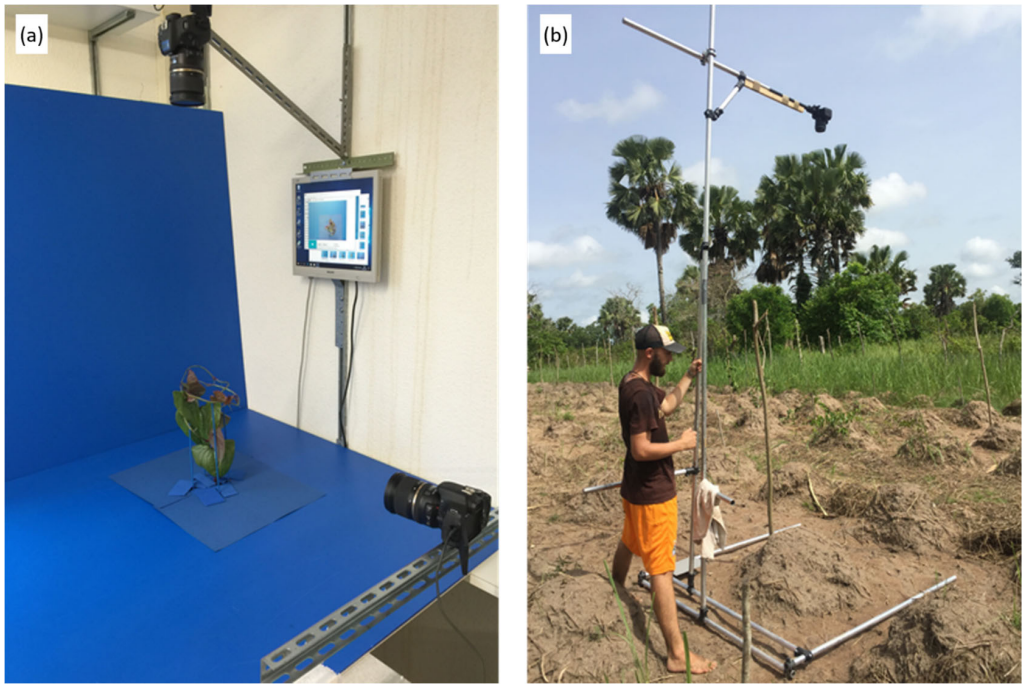

Figure 1. (**a**) Indoor imaging station with two cameras used for yam imaging at ETH Zurich plant research station in Eschikon and (**b**) the field-imaging platform with one camera in nadir view as moved over the field by the imaging operator in Côte d'Ivoire.

For image acquisition, both cameras were simultaneously triggered with a software (DSLR remote multi-camera software, Breeze systems Ltd., Knoll House, Knoll Road, Camberley, Surrey GU15 3SY, UK). The cameras were set to the P-mode for imaging meaning that the camera was setting automatically shutter speed and aperture according to light conditions. The camera ISO was set to 200 and automatic focus was used. We used manual focus only during very early stages of plant growth, when leaf area was insufficient to satisfy the auto focus algorithm. Metering mode was set to center-weighted average focusing on the center of the picture, where plants were located. All other settings were left as standard settings.

Imaging of plants took place at 20, 40 and 61 days after emergence and included the recording of three images, one nadir (top view) perspective and two side view perspectives with a 90° horizontal rotation to capture two different view angles on the plant shape. The traits of interest were compared to projected leaf surface measured by imaging with the nadir view, side view 1 (0°), side view 2 (90°), the sum of two views (nadir and side 1) and with the sum of the three views.

2.3.2. Imaging in the Field Experiment

For field image acquisition an RGB camera (Canon EOS 400D, Tokyo, Japan) with a fixed focal length lens (Canon EF 35 mm f/2 IS USM lens) was used. The camera was mounted on a self-constructed manually moveable field camera post made of aluminum pipes and connectors (Figure 1b) inspired from a device constructed by Grieder et al. [34]. The post can be disassembled and transported easily. The camera was mounted on top of the post and images were taken from a nadir position from a height of 4 m using a remote release cable. The area of interest (AoI) used for image processing is bordered by two aluminum pipes on the left and right side at the base of the post. In the left bottom corner of this area a grey reference panel with known reflection properties (ca. 25%) (Kömatex, light grey) was attached for radiation correction of the images.

Because of bad weather conditions, imaging only started on 5 July 2018 and was continued until 10 August 2018. It was carried out on the two same representative plants per plot. Images were recorded with the manual exposure mode allowing to fix the aperture and shutter speed. The ISO was usually set to 100 and increased to 200 on cloudy days. Shutter speed and aperture were adjusted for each imaging campaign doing test images on the field and checking the average histogram for color intensities. As soon as the aperture and shutter speed fitted the light conditions, the camera was mounted on the field camera post and the position of the camera was carefully adjusted to point at the AoI.

Imaging was carried out after placing the post above the plant (nadir view for the camera) using a remote trigger taking one image per plant. Afterwards, the post was moved to the next plant and so forth. Imaging of the plants in the experimental field was carried out always in the same order to allow automated handling during post processing and analysis.

2.3.3. Image Processing and Analysis in the Greenhouse and Field Experiment

For indoor imaging, reference images without any plant were taken before each imaging series to correct for light and lens distortion. These reference images included a full blue screen image from both nadir and side view perspectives and a full screen recording of a checkerboard with known square edge length of 50 mm (Figure 2a). This procedure was repeated before each imaging campaign. The rectification for lens distortion and light variation was done using a custom-made Matlab script using recorded reference images. After rectification, the images were segmented using an in-house tool. The generated outputs were a black and white image (mask) with plant material separated from the background and plant pixels that were counted for projected area measurements allowing for leaf surface calculation (Figures 2d and 3c). Color thresholds that separate the blue band were adjusted for each series of top- or side view images to allow best segmentation. For some series, the saturation was additionally adjusted. For this case, low saturation was also excluded during analysis because of high light intensities and reflection occurring on the blue plates. Plant images taken from the nadir and side perspectives allowed to measure the number of pixels in shoots giving the projected leaf surface (Figure 3), while images taken from the nadir perspective of separated and spread out leaves provided the total leaf surface (without overlapping) (Figure 2b,c).

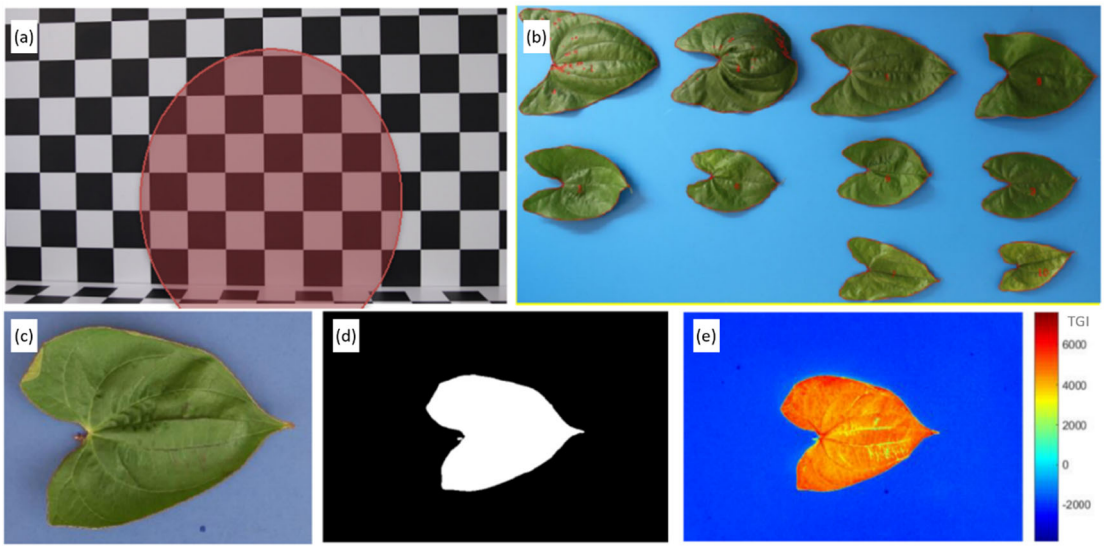

Figure 2. (**a**) Checkerboard for distortion correction; (**b**) leaves spread out on the blue plate; (**c**) single leaf; (**d**) segmented leaf; and (**e**) single leaf triangular greenness index, TGI. Red dots on leaves (**b**) indicate saturated pixels or necrotic tissue not identified as green and excluded from the spectral index analysis.

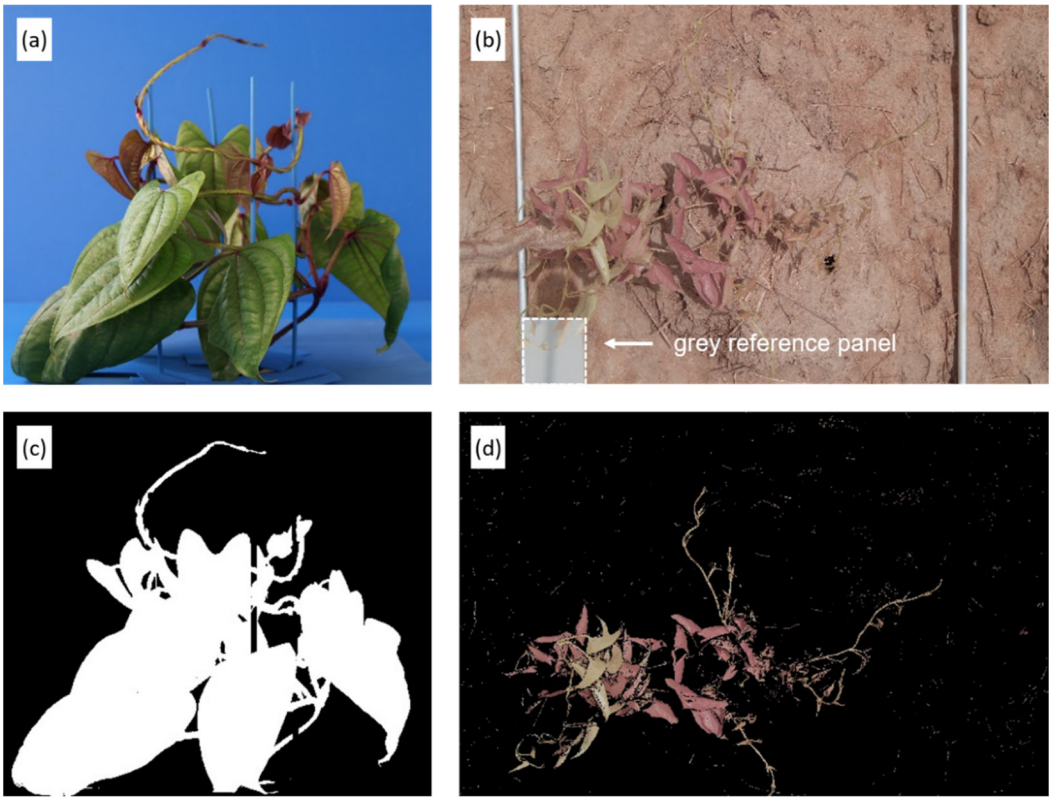

Figure 3. (**a**) Side view image of a yam plant in the indoor imaging platform; (**b**) nadir image from the field imaging platform and the corresponding segmented images (**c**,**d**), respectively.

The triangular greenness index (TGI) makes use of the differences between reflectance in the red (r), green (g) and blue (b) camera channels by calculating the area spanning between the three points in the spectra as follows [10]:

$$TGI = -0.5 \times [(W670 - W480) \times (Rr - Rg) - (W670 - W550) \times (Rr - Rb)] \quad (1)$$

With W670, W480, W550 being the center wavelengths in nm; Rr, Rg, and Rb are the reflectance values for the three camera bands (r, 630–690 nm, g, 520–600 nm and b, 450–520 nm), respectively. In the glasshouse the TGI values were derived from nadir-recorded images of separated leaves and averaged at plant level (Figure 2e). Due to the calculation scheme of this index, dark green leaf regions have rather low TGI values, whereas yellow-green leaf regions are characterized by high TGI values (i.e., high chlorophyll content leads to low TGI value).

RGB images taken in the field experiment were analyzed with the same Matlab script that was used for plants grown in the greenhouses. Images taken with the field imaging platform were cropped to the target area inside the two aluminum pipes of the field camera post base. Correction of images for light conditions was done using a grey reference plate as described above. The targeted area was segmented for vegetation using the self-learning EasyPCC program developed by Guo et al. [35], allowing to count vegetation and background pixels separately. EasyPCC is a software using a decision-tree-based segmentation model (DTSM). In several images with diverse light conditions, plant material and background had to be marked manually to train the program to perform a robust segmentation on the complete data set. The generated DTSM included nine different color features based on which single pixels were then categorized into vegetation or background [36]. Soil surface cover by yam was calculated as the ratio between the plant shoot pixels to the total number of pixels in 1 m^2, as we had a planting density of one plant per m^2. In the field experiment, the TGI was derived from the vegetation pixels.

2.4. Statistics

Statistical analysis was performed using RStudio (Version 1.0.143, 2009–2016 RStudio, Inc. 250 Northern Ave, Boston, MA 02210, USA). Analysis of variance (ANOVA) was performed followed by a Fisher's least significance test (LSD-posthoc test) to analyze for treatment effects in the greenhouse experiment. Data were checked for normal distribution by regarding the scale location, constant leverage, fitted values and normal Q-Q plots. All investigated data were normally distributed and thus were analyzed without transformation. The correlation between variables was assessed by calculating Pearson's correlation coefficients followed by linear regression analysis.

3. Results

3.1. Greenhouse Experiment

Data describing plant growth and N leaf content in the greenhouse experiment are presented in the Supplementary Materials (Figures S1 and S2, Table S1). Table 1 shows that the projected leaf surface measured as the number of pixels from different points of view was highly significantly related with the traits of interest (total leaf surface, total fresh and dry weight, number of leaves and total stem length). The nadir view alone provided already excellent results. The coefficient of correlations between number of pixels (projected leaf surface) and traits of interest improved slightly with the sum of two views, while the sum of three views did not perform better than that of two views.

Table 1. Pearson's correlation coefficients between projected leaf area measured with the nadir view, side view 1 (0°) and 2 (90°), the sum of two views (nadir and side view 1) and the sum of three views and total leaf area, total fresh and dry weight, number of leaves and total stem length of water yam cv raja ala grown in a greenhouse during 20, 40 and 61 days after emergence in the presence of different N fertilization rates. *** Denotes significance responses on *p*-values 0.001 (n = 60 plants for each correlation).

Projected Leaf Surface	Total Leaf Surface	Total Shoot Fresh Weight	Total Shoot Dry Weight	Number of Leaves	Total Stem Length
Pixels Plant^{-1}	**cm^2 Plant^{-1}**	**g Plant^{-1}**		**Leaves Plant^{-1}**	**cm Plant^{-1}**
Nadir view	0.92 ***	0.95 ***	0.94 ***	0.85 ***	0.82 ***
Side 1 (0°)	0.95 ***	0.96 ***	0.96 ***	0.92 ***	0.86 ***
Side 2 (90°)	0.93 ***	0.95 ***	0.94 ***	0.90 ***	0.83 ***
Sum of 2 images	0.95 ***	0.97 ***	0.96 ***	0.92 ***	0.86 ***
Sum of 3 images	0.95 ***	0.96 ***	0.96 ***	0.92 ***	0.85 ***

The relations between the projected leaf surface measured from the nadir view and total aboveground fresh weight and total leaf area are shown in Figure 4. Whereas the variation in projected leaf surface were well explained by the variation in total shoot fresh weight or total leaf surface at 20 and 40 days after emergence, points measured after 61 days of emergence showed a higher variability.

The TGI values were highly significantly correlated to SPAD values measured on the 7th leaf, (Figure 5) and to the N content in the 1st and 7th fully developed leaves (Figure 6). The points from the 20 days after emergence sampling showed for both types of leaves a higher variability around the model compared to the points obtained at 40 and 61 days after emergence (Figure 6).

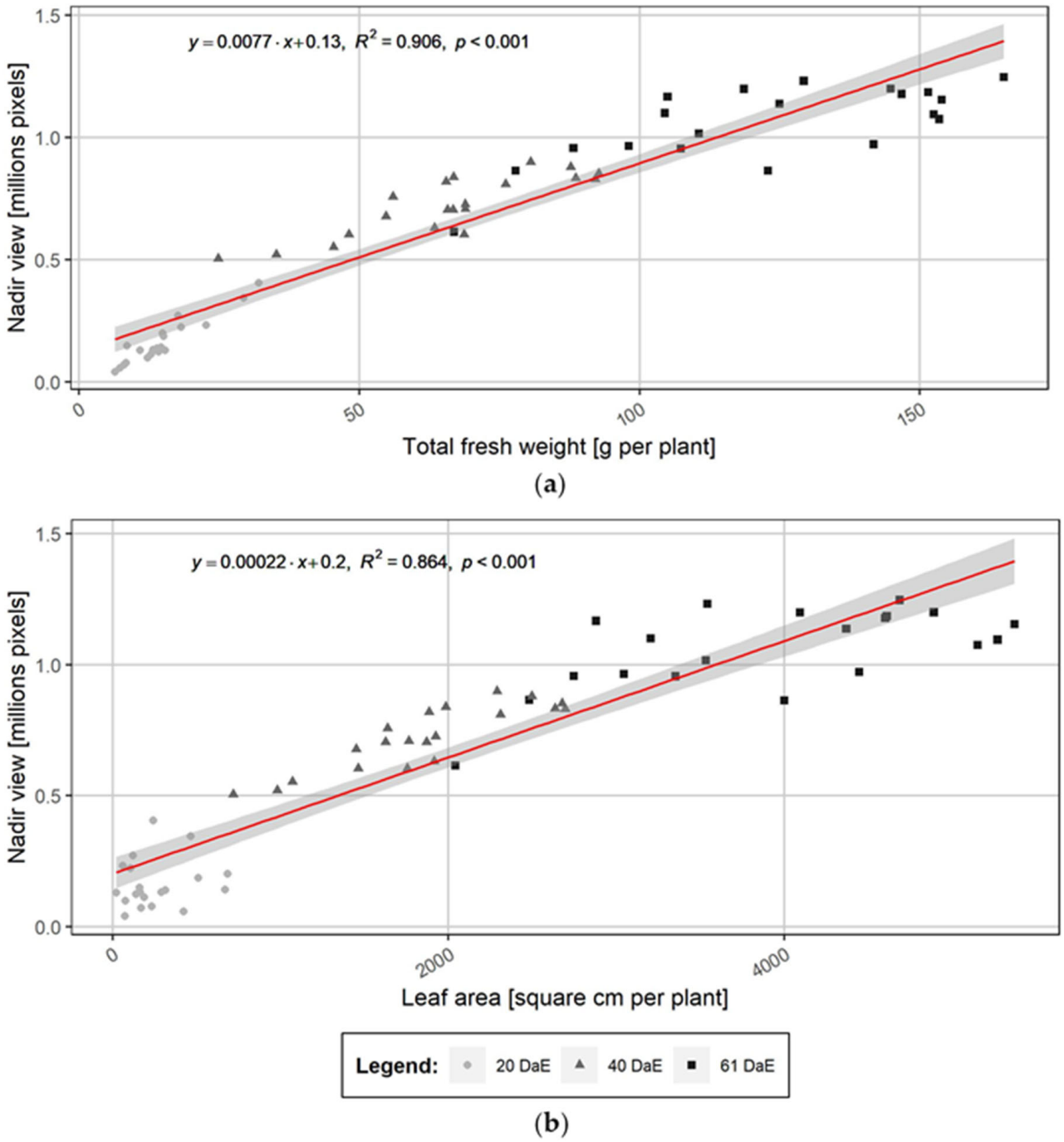

Figure 4. Linear regressions: (**a**) between the projected leaf surface measured from the nadir view (in millions of pixels) and total shoot fresh weight (g plant^{-1}); and (**b**) between the projected leaf surface measured from the nadir view (in millions of pixels) and total leaf surface (cm^2 per plant) of water yam (cv raja ala) grown in a greenhouse in the presence of different N fertilization rates. The linear regressions, the coefficients of determination (R^2) and the p values are shown on each graph. The form of the symbols indicates the sampling dates: 20, 40 and 61 days after emergence (DaE) (n = 60 plants for both figures). The grey band indicates the 95% confidence interval.

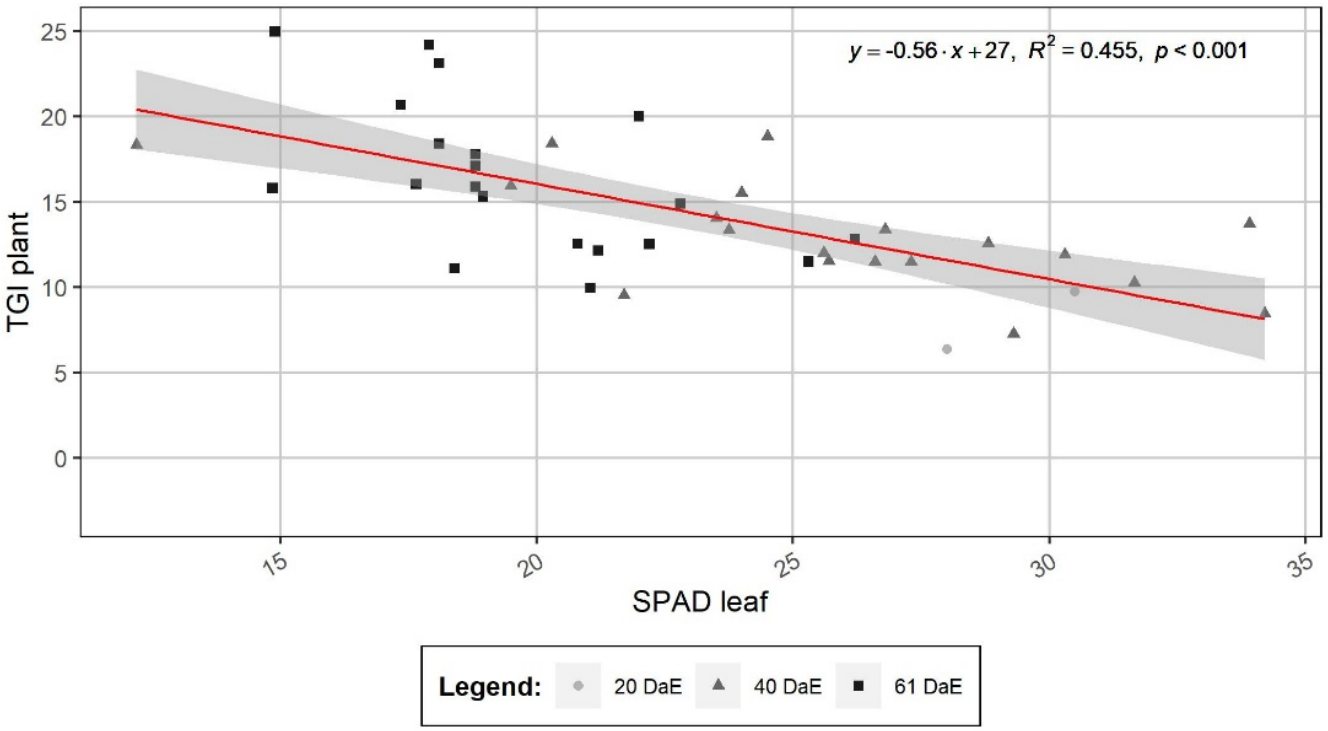

Figure 5. Relationship between the SPAD value measured on the 7th fully developed leaf starting from the apex of the main vine and the plant TGI value averaged for all leaves at 20, 40 and 61 days after emergence, DaE) in a greenhouse experiment conducted with water yam cv raja ala grown in the presence of different N fertilizations. Each dot represents the value for one plant (n = 42 plants). The form of the symbols indicates the sampling dates, and the grey band indicates the 95% confidence interval.

3.2. Field Experiment

Soil surface cover (SSC) with yam shoots between 5 July and August 10 increased in average from 3.0% to 19.6% (Figure 7, Table S4 in Supplementary Materials). These changes could be modelled as highly statistically significant linear functions of time for each single plant (SSC = a * day + b) with $R^2 > 0.88$, and $p < 0.01$. As the field experiment included many treatments without replicate, we decided to present the changes in the factor a (% of SSC/day) in an aggregated manner, showing either the effect of fertilization using the various rotations as pseudo-replicates, or the effect of rotation using different fertilization as pseudo-replicates (Table S5 in Supplementary Materials). The lower factor a observed in the non-fertilized treatment (T0) suggests that yam shoots were covering the soil less rapidly in this treatment compared to the fertilized treatments. Similarly, the lower factor a observed in the rotation R3 (intercropped yam/maize—rice—yam rotation) suggests that yam shoots were covering the soil less rapidly in this treatment compared to the other rotation treatments.

The average a values calculated on each of the 16 plots were weakly positively linearly correlated (R^2 = 0.27, p value of 0.0357) to the final tuber yields estimated in nearby plots and submitted to the same treatments (see yields in Table S3 and correlation in Figure S6 in the Supplementary Materials).

A significant nonlinear relation was observed between the average TGI values calculated for each sampling day and the number of days after germination (Figure 8).

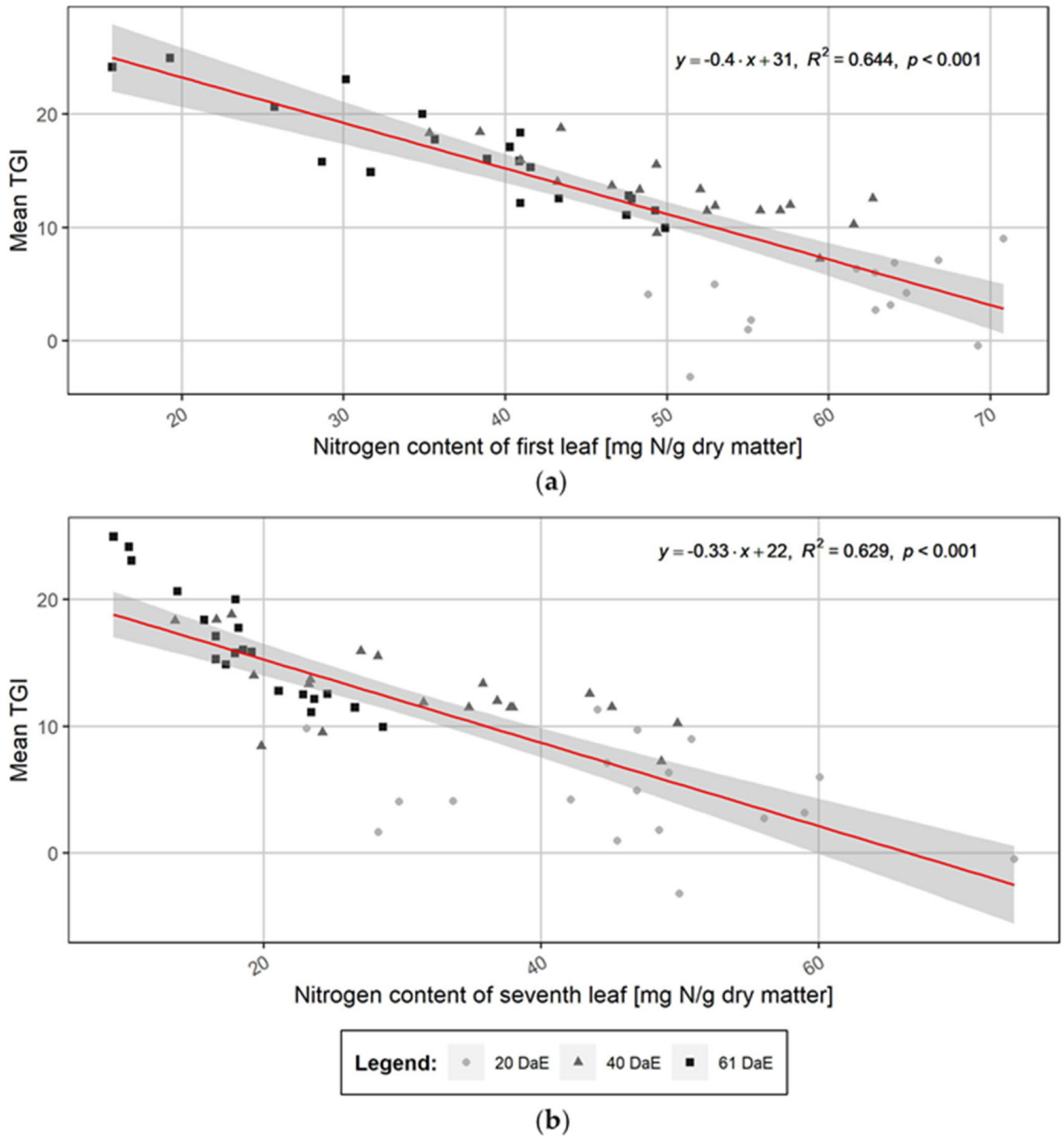

Figure 6. Relationships between the mean TGI measured at plant level and: (**a**) the N content of the 1st fully developed leaf located at the apex of the main vine (n = 52 plants); and (**b**) the N content of the 7th fully developed leaf starting from the apex of the main vine (n = 58 plants) in water yam cv raja ala grown in the presence of different N fertilizations and sampled at 20, 40 and 61 days after emergence (DaE). The form of the symbols indicates the sampling dates, and the grey band indicates the 95% confidence interval.

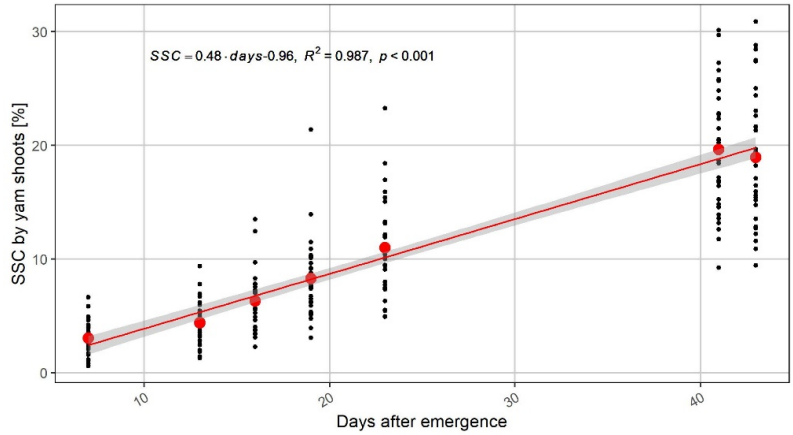

Figure 7. Relationship between the proportion of soil surface cover by yam shoots (SSC expressed in %) derived from the number of plant pixels measured in TGI images and average over all the plants and time (days after 80% of emergence) in a field experiment conducted with water yam (cv C18) in Tieningboué (Côte d'Ivoire). Each dot represents the value per plant and red dots represent the average values for all 32 plants. The grey band indicates the 95% confidence interval.

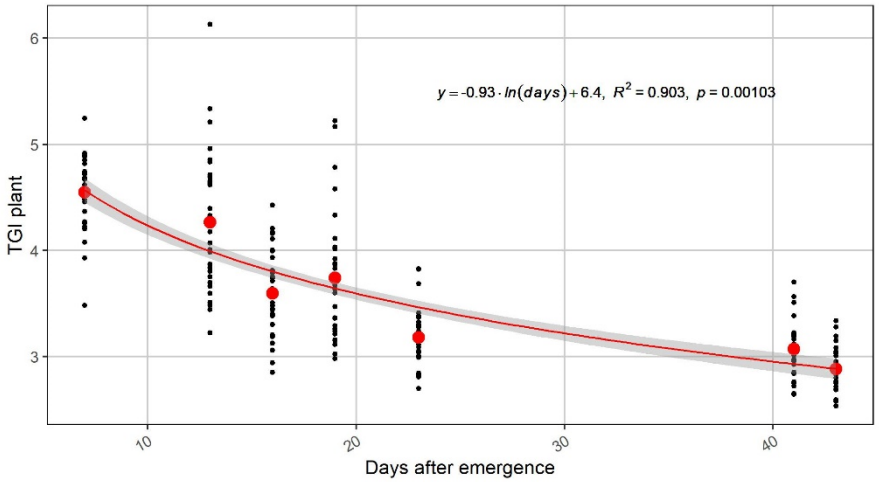

Figure 8. Relationship between the TGI of plants measured by imaging with an RGB camera and time (days after germination) in a field experiment conducted with water yam (cv C18) in Tieningboué (Côte d'Ivoire) with different fertilizations and rotations. Each dot represents the value per plant and red dots represent the average values for all 32 plants. The grey band indicates the 95% confidence interval.

The SPAD values measured on 14 July and 8 and 10 August 2018 on diagnostic leaves was negatively correlated to the TGI values measured at plant level (Figure 9; Table S6), whereas no relation was observed between TGI and leaf N content, or SPAD and leaf N content measured on 8 and 10 August 2018.

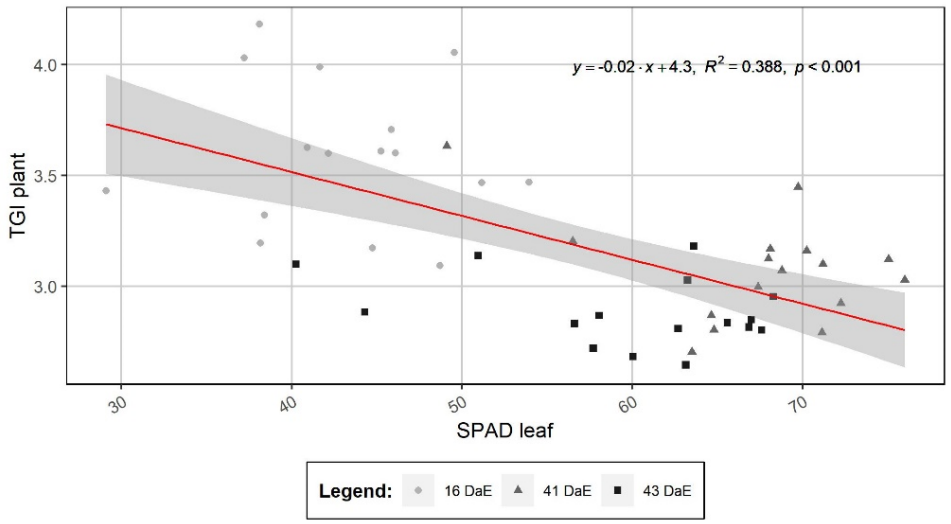

Figure 9. Relationship between the SPAD value measured on diagnostic leaves with an RGB camera and TGI of plants measured by imaging and time on 14 July, 8 and 10 August (after 16, 41 and 43 days after emergence, DaE) in a field experiment conducted with water yam (cv C18) in Tieningboué (Côte d'Ivoire) with different fertilizations and rotations. Each dot represents the average values for one plot or two plants. The grey band indicates the 95% confidence interval.

4. Discussion

The results presented above and in the Supplementary Material for the glasshouse study conducted by Müller [23], show that the fixed indoor phenotyping station yielded results that robustly reflected the impact of N fertilization rates on early plant growth, and on leaf SPAD values and N content. In her glasshouse study Ringger [22] also showed that indoor imaging allowed predicting total leaf area, and biomass production in two yam cultivars raja ala and florido (Table S2 in Supplementary Materials; Figure S3 in Supplementary Materials). Furthermore, she showed significant relations between SPAD values and N leaf content and between TGI values and N leaf content for the cultivar raja ala (Figure S4 in Supplementary Materials) used by Müller [23] but not for the cultivar florido (results not shown). Finally, the mobile imaging of yam in the field experiment showed an increase in soil surface cover by yam shoots and a decrease of plant TGI with time. Image-based phenotyping seems therefore to generate results that are relevant for describing the early growth of yam. The discussion will touch on the limits and interests of image-based phenotyping, and on the perspective this technique offers for yam research.

4.1. Imaging for Assessing Yam Growth

In the greenhouse, it was necessary to stack and wind the shoots around the sticks to transport plants to the imaging station. This has likely limited the sensitivity of the quantification of leaf surface especially for plants with many leaves. Indeed, better coefficients of correlation were observed between the sums of pixels (i.e., the projected leaf surface) obtained from two images (nadir view plus one side view) and the measured plant traits (total leaf surface and biomass) than between the single nadir view and these plant traits. Furthermore, the relations between these plant traits and the number of pixels obtained from the nadir view were less tight for the plants grown during 61 days after emergence than for younger plants, which was probably due to the higher number of leaves and to more leaves overlapping each other for the older plants. The nadir view alone nevertheless already reflected very well plant growth traits and the differences induced by N fertilization on these traits. These results therefore suggest that stacking and winding plants for imaging had no major negative impact on the imaging results until 61 days after emergence.

Nadir imaging in the field showed that the soil surface cover by yam shoots increased linearly with time until seven weeks after emergence. This result is in agreement with the linear increase of leaf area index observed from 50 to 100 days after emergence with an improved water yam cultivar by Diby et al. [3]. In this last work however, soil surface coverage by yam foliage reached 20% to 40% 52 days after planting [3], whereas 5% to 23% soil surface cover were observed in our field experiment at 52 days after planting (23 days after emergence). This suggests either that these two yam cultivars had different growth habits, or that plant growth was limited in our field experiment.

A weak but significant positive correlation was observed between the rate of soil surface cover by yam shoots during the first 43 days and the final tuber yield. This agrees with earlier works which found that early yam emergence and growth is positively related to tuber yield at plant level [6] but this relation needs to be validated in further field experiments.

4.2. Imaging for Assessing Chlorophyll and N Leaf Contents in Yam

The significant negative correlation observed between SPAD and TGI in the greenhouse for the cultivar raja ala [23] was in principle expected as both techniques use leaf spectral properties related to light absorption and reflectance by chlorophylls [10]. This was however an interesting result as the SPAD value was only measured on the 7th fully developed leaf counted from the apex while TGI was measured on all leaves and averaged. Similarly, we observed a negative correlation between the SPAD values measured on diagnostic leaves (between the 6th and 8th leaves from the apex) and the TGI measured at canopy level in the field on cultivar C18. Similar correlations have observed e.g., by Hunt et al. [37] on rye. These correlations suggest therefore that TGI values measured either on separated leaves or at canopy level provide relevant information on chlorophyll content in yam plants.

Our two glasshouse studies [22,23], conducted with the cultivar raja ala under similar conditions, showed significant relationships between leaf N content and SPAD and TGI values, whereas no relations were observed between these parameters in the field experiment for the cultivar C18. No relation between leaf N content and SPAD and TGI values could be found for the cultivar florido in the glasshouse either [22]. The relation between chlorophyll (measured with SPAD or TGI) and N leaf contents is indeed complex as it strongly depends on genetic × environment × management interactions [28]. Genetic, environment and management affect leaf properties in yam as e.g., leaf color depends on the cultivar, while leaf thickness is modified by shade [38] and leaf N content by fertilization. We suggest nevertheless that further work should be conducted on the relationships between TGI, SPAD and N leaf content to assess the usefulness of these nondestructive techniques for improved N management in yam as this has been shown for cereals [39].

4.3. Perspectives

The results obtained in this study are an important first step towards field use of imaging techniques in yam research. They show the potential of such methods to detect increase in biomass and changes in leaf composition. Yet, they need to be validated for longer growth duration in the field. Moreover, it is necessary to test these techniques in different genetic x environment x management conditions by testing other important species such as white yam, air yam, and lesser yam, in different rotations, submitted to different fertilization regimes and in different pedo-climatic conditions.

The use of such imaging techniques will be useful to adapt yam cropping systems to local conditions. Indeed, given the diversity of yam cropping systems [1] there is no one suits all solution [2,4]. Appropriate site-specific innovations need to be designed, tested, and validated with local stakeholders [4]. If this is done, there is a chance that farmers will adopt innovations to sustainably improve yam productivity in their fields [2].

Supplementary Materials: The following are available online at https://www.mdpi.com/2073-4395/11/2/249/s1, Figure S1: Changes with time in: (a) total aboveground fresh weight in g per

plant; (b) total aboveground dry weight in g per plant; (c) total stem length in cm per plant; and (d) total number of leaves per plant in water yam (cv raja ala) grown for 61 days after emergence in a greenhouse in the presence of different N inputs. Each column represents the average measured for 20 plants, the bars show the standard deviation, Table S1: Effect of N fertilization on total aboveground fresh weight (in g per plant) of water yam (cv raja ala) grown for 20, 40 and 61 days after emergence in a greenhouse. Different letters within a column indicate significant differences according to a Fisher's least significance test at p-level ≤ 0.05 (n = five plants per treatment), Figure S2: Nitrogen concentrations in: the 1st (a); and 7th (b) fully developed leaves sampled from the apex of the main vine after three, six and nine weeks after germination (20, 40 and 61 days after emergence) in water yam (cv raja ala) grown in a greenhouse in the presence of different N fertilization rates. Columns show the average and the bar the standard deviation values. Letters denote significant differences calculated with least significant difference (LSD) test at p-level ≤ 0.05 (n = five plants per column), Table S2: Pearson's correlation coefficient of projected leaf area assessed from the nadir (top) view, side view 0°, side view 90°, the sum of two views (nadir and side 0°) and the sum of three views and destructively measured total leaf area, dry weight and fresh weight measured on two genotypes of water yam (raja ala and florido, n = 24 genotype^{-1}) grown in the greenhouse under three nitrogen fertilizer treatments (0, 50 and 170 kg N ha^{-1}) and harvested six and eight weeks after emergence. Leaf area was transformed prior to the calculation using the natural logarithm, Figure S3: Relation between projected leaf surface calculated from single top (nadir) images, and destructively measured: total leaf surface (a); shoot dry weight (b); and shoot fresh weight (**c**) for two genotypes of water yam (SL, CI, n = 24 genotype^{-1}) grown in the greenhouse under three nitrogen fertilizer treatments (0, 50 and 170 kg N ha^{-1}) and harvested six and eight weeks after emergence, Figure S4: Relation between SPAD value and leaf nitrogen (N) content at different leaf positions (leaf no. 1, 8, 16, counted from base to apex): (a) and between TGI value (triangular greenness index) and leaf nitrogen (N) content at different leaf positions (leaf no. 1, 8, 16, counted from base to apex); (b) in water yam cv raja ala, six and eight weeks after emergence (wae). Plants were grown under three nitrogen treatments (0, 50, 170 kg N ha^{-1}) in a greenhouse. Regression lines were included, when results were significant (p-value ≤ 0.05), Figure S5: Climate diagram of the season 2018 for Tieningboué. The mean temperature (°C) is shown by the red line, the maximum temperature by the upper black line and the minimum temperature by the lower black line. The precipitation (mm) is shown with bar plots. No weather data was available for 22 days in March and 22 days in April 2018, Table S3: Tuber yield (average and standard error) of water yam cv C18 measured in a nearby experiment located on the same soil and submitted to the same treatments (rotation R1 to R4 and fertilization T0 to T3, see details in the paper) as those studied in our field experiment, Table S4: Soil surface coverage (%) measured from pixel numbers obtained from TGI image for each studied plant between 5 July 2018 and 10 August 2018 in our field experiment, Table S5: Average and standard deviation values of the slope (a, expressed in SSC day^{-1}) of the linear equations describing the changes in soil surface cover by yam shoots with time between 5 July and 10 August for the various fertilization and rotation treatments implemented in a field experiment conducted with water yam (cv C18) in Tieningboué (Côte d'Ivoire). Each treatment has a n = 8 plants. Due to the absence of replicate, it was not possible to analyze these data statistically, Figure S6: Relationship between final tuber yields (t tuber ha^{-1}) and the average daily rate of soil surface coverage by yam shoots (a, expressed in SSC day^{-1}) between 5 July 2018 and 10 August 2018 in our field experiment, Table S6: TGI measured at plant level for each studied plant between 5 July 2018 and 10 August 2018 in our field experiment.

Author Contributions: Conceptualization, E.F. and F.L.; imaging methodology, F.L., N.K. and A.W.; software, N.K. and A.W.; greenhouse house experiments, C.R. and L.M.; field experiment, L.M., N.P., V.K.H. and D.I.K.; writing—original draft preparation, E.F. and F.L.; writing—review and editing, all authors; visualization, L.M. and C.R.; supervision, E.F., F.L., V.K.H. and D.I.K.; project administration, E.F.; funding acquisition, E.F. All authors have read and agreed to the published version of the manuscript.

Funding: This research was funded in the frame of the food security module of the "Swiss program for research on global issues for development" by the SNF and the SDC (YAMSYS project, SNF project number: 400540_152017/1).

Institutional Review Board Statement: Not applicable.

Informed Consent Statement: Not applicable.

Data Availability Statement: The data are available on request to the first authors (Frossard E. and Liebisch F) of this publication.

Acknowledgments: The authors warmly thank Monika Macsai, and Laurie Schönholzer from the group of plant nutrition of the ETH and Brigitta Herzog from the group of crop science of ETH for their support in the greenhouse experiments as well as the members of the YAMSYS field crew in Tieningboué for their help.

Conflicts of Interest: The authors declare no conflict of interest. The funder had no role in the design of the study; in the collection, analyses, or interpretation of data; in the writing of the manuscript, or in the decision to publish the results.

References

1. Lebot, V. *Tropical Root and Tuber Crops; Cassava, Sweet Potato, Yams and Aroids*, 2nd ed.; CABI: Wallingford, UK, 2020.
2. Frossard, E.; Aighewi, B.; Aké, S.; Barjolle, D.; Baumann, P.; Bernet, T.; Dao, D.; Diby, L.N.; Floquet, A.; Hgaza, V.K.; et al. The challenge of improving soil fertility in yam cropping systems of West Africa. *Front. Plant Sci. Agroecol. Land Use Syst.* **2017**, *8*, 1953. [CrossRef] [PubMed]
3. Diby, L.N.; Hgaza, V.K.; Tié, T.B.; Assa, A.; Carsky, R.; Girardin, O.; Sangakkara, U.R.; Frossard, E. How does soil fertility affect yam growth? *Acta Agric. Scand. B Soil Plant Sci.* **2011**, *61*, 448–457. [CrossRef]
4. Kiba, D.I.; Hgaza, V.K.; Aighewi, B.; Aké, S.; Barjolle, D.; Bernet, T.; Diby, L.N.; Ilboudo, L.J.; Nicolay, G.; Oka, E.; et al. A transdisciplinary approach for the development of sustainable yam (*Dioscorea* spp.) production in West Africa. *Sustainability* **2020**, *12*, 4016. [CrossRef]
5. Cornet, D.; Sierra, J.; Tournebize, R.; Ney, B. Yams (*Dioscorea* spp.) plant size hierarchy and yield variability: Emergence time is critical. *Eur. J. Agron.* **2014**, *55*, 100–107. [CrossRef]
6. Cornet, D.; Sierra, J.; Tournebize, R.; Gabrielle, B.; Lewis, F.I. Bayesian network modeling of early growth stages explains yam interplant yield variability and allows for agronomic improvements in West Africa. *Eur. J. Agron.* **2016**, *75*, 80–88. [CrossRef]
7. Hgaza, V.K.; Oberson, A.; Kiba, D.I.; Diby, L.N.; Aké, S.; Frossard, E. The nitrogen nutrition of yam (*Dioscorea* spp). *J. Plant Nutr.* **2020**, *43*, 64–78.
8. Buerkert, A.; Lawrence, P.R.; Williams, J.H.; Marschner, H. Nondestructive measurements of biomass in millet, cowpea, groundnut, weeds and grass swards using reflectance, and their application for growth analysis. *Exp. Agric.* **1995**, *31*, 1–11. [CrossRef]
9. Buerkert, A.; Mahler, F.; Marschner, H. Soil productivity management and plant growth in the Sahel: Potential of an aerial monitoring technique. *Plant Soil* **1996**, *180*, 29–38. [CrossRef]
10. Hunt, E.R.; Daughtry, C.S.T.; Eitel, J.U.H.; Long, D.S. Remote sensing leaf chlorophyll content using a visible band index. *Agron. J.* **2011**, *103*, 1090–1099. [CrossRef]
11. Kirchgessner, N.; Liebisch, F.; Yu, K.; Pfeifer, J.; Friedli, M.; Hund, A.; Walter, A. The ETH field phenotyping platform FIP: A cable-suspended multi-sensor system. *Funct. Plant Biol.* **2017**, *44*, 154–168.
12. Joalland, S.; Screpanti, C.; Gaume, A.; Walter, A. Belowground biomass accumulation assessed by digital image based leaf area detection. *Plant Soil* **2016**, *398*, 257–266. [CrossRef]
13. Joalland, S.; Screpanti, C.; Liebisch, F.; Varella, H.V.; Gaume, A.; Walter, A. Comparison of visible imaging, thermography and spectrometry methods to evaluate the effect of *Heterodera schachtii* inoculation on sugar beets. *Plant Methods* **2017**, *13*, 73. [CrossRef] [PubMed]
14. Li, B.; Xu, X.; Han, J.; Zhang, L.; Bian, C.; Jin, L.; Liu, J. The estimation of crop emergence in potatoes by UAV RGB imagery. *Plant Methods* **2019**, *15*, 15. [CrossRef] [PubMed]
15. Hunt, E.R.; Horneck, D.A.; Spinelli, C.B.; Turner, R.W.; Bruce, A.E.; Gadler, D.J.; Brungardt, J.J.; Hamm, P.B. Monitoring nitrogen status of potatoes using small unmanned aerial vehicles. *Precis. Agric.* **2018**, *19*, 314–333. [CrossRef]
16. Liebisch, F.; Kirchgessner, N.; Schneider, D.; Walter, A.; Hund, A. Remote, aerial phenotyping of maize traits with a mobile multi-sensor approach. *Plant Methods* **2015**, *11*, 9. [CrossRef]
17. Makino, A.; Sakuma, H.; Sudo, E.; Mae, T. Differences between Maize and Rice in N-use Efficiency for Photosynthesis and Protein Allocation. *Plant Cell Physiol.* **2003**, *44*, 952–956. [CrossRef]
18. Iseki, K.; Matsumoto, R. Non-destructive shoot biomass evaluation using a handheld NDVI sensor for field-grown staking Yam (*Dioscorea rotundata* Poir.). *Plant Prod. Sci.* **2019**, *22*, 301–310. [CrossRef]
19. Kolade, O.A.; Oguntade, O.; Kumar, L. Screening for resistance to Yam Anthracnose Disease. Virology/Germplasm Health Unit, IITA Ibadan: Ibadan, Nigeria, 2018. Available online: https://africayam.org/download/screening-resistance-yam-anthracnose-disease/ (accessed on 24 September 2020).
20. Ramcharan, A.; Baranowski, K.; McCloskey, P.; Ahmed, B.; Legg, J.; Hughes, D.P. Deep Learning for Image-Based Cassava Disease Detection. *Front. Plant Sci.* **2017**, *8*, 1852. [CrossRef]
21. Darkwa, K.; Olasanmi, B.; Asiedu, R.; Asfaw, A. Review of empirical and emerging breeding methods and tools for yam (*Dioscorea* spp.) improvement: Status and prospects. *Plant Breed.* **2020**, *139*, 474–497. [CrossRef]
22. Ringger, C. Development of a digital method to assess shoot development of yam (*Dioscorea* spp.) at early vegetative stage. Master's Thesis, ETH Zürich, Zürich, Switzerland, 9 September 2018.

23. Müller, L. Digital Phenotyping of Yam (*Dioscorea* sp.) under Glasshouse and Field Conditions. Master's Thesis, Eth Zürich, Zürich, Switzerland, 21 November 2017.
24. Aighewi, B.A.; Maroya, N.G.; Asiedu, R. *Seed Yam Production from Minisetts: A Training Manual*; International Institute for Tropical Agriculture: Ibadan, Nigeria, 2014.
25. O'Sullivan, J.N.; Jenner, R. Nutrient deficiencies in greater yam and their effects on leaf nutrient concentrations. *J. Plant Nutr.* **2006**, *29*, 1663–1674. [CrossRef]
26. Wang, Y.; Wang, D.; Shi, P.; Omasa, K. Estimating rice chlorophyll content and leaf nitrogen concentration with a digital still color camera under natural light. *Plant Methods* **2014**, *10*, 36. [CrossRef] [PubMed]
27. Markwell, J.; Osterman, J.C.; Mitchell, J.L. Calibration of the Minolta SPAD-502 leaf chlorophyll meter. *Photosyn. Res.* **1995**, *46*, 467–472. [CrossRef] [PubMed]
28. Friedman, J.M.; Hunt, E.R.; Mutters, R.G. Assessment of leaf color chart observations for estimating maize chlorophyll content by analysis of digital photographs. *Agron. J.* **2016**, *108*, 822–829. [CrossRef]
29. Hgaza, V.K.; Diby, L.N.; Aké, S.; Frossard, E. Leaf growth and photosynthetic capacity as affected by leaf position, plant nutritional status and growth stage in *Dioscorea alata* L. *J. Anim. Plant Sci.* **2009**, *5*, 483–493.
30. Müller, P. Measurement of Leaf Surface Area, Soil Cover and N Content in Leaves of Field-Grown Yams (*Dioscorea* spp). Master's Thesis, ETH Zürich, Zürich, Switzerland, 7 Januray 2019.
31. WRB. *International Soil Classification System for Naming Soils and Creating Legends for Soil Maps*; FAO World Soil Resource Reports; FAO: Roma, Italy, 2014.
32. Schneider, K. *Soil Characterization of YAMSYS Sites*; Internal YAMSYS Report; ETH: Zürich, Switzerland, 2018.
33. Doumbia, S.; Koko, L.; Aman, S.A. L'introduction et la diffusion de la variété d'igname C18 en région centre de Côte d'Ivoire. *J. Appl. Biosci.* **2014**, *80*, 7121–7130. [CrossRef]
34. Grieder, C.; Hund, A.; Walter, A. Image based phenotyping during winter: A powerful tool to assess wheat genetic variation in growth response to temperature. *Funct. Plant Biol.* **2015**, *42*, 387–396. [CrossRef]
35. Guo, W.; Zheng, B.; Duan, T.; Fukatsu, T.; Chapman, S.; Ninomiya, S. EasyPCC: Benchmark Datasets and Tools for High-Throughput Measurement of the Plant Canopy Coverage Ratio under Field Conditions. *Sensors* **2017**, *17*, 798. [CrossRef]
36. Thenkabail, P.S.; Lyon, J.G. *Hyperspectral Remote Sensing of Vegetation*, 1st ed.; CRC Press: Boca Raton, FL, USA, 2012. [CrossRef]
37. Hunt, E.R.; Daughtry, C.S.T.; Mirsky, S.B.; Hively, S.B. Remote Sensing with Simulated Unmanned Aircraft Imagery for Precision Agriculture Applications. *IEEE J. Sel. Top. Appl. Earth Obs. Remote Sens.* **2014**, *7*, 4566–4571. [CrossRef]
38. Onwueme, I.C.; Johnston, M. Influence of shade on stomatal density, leaf size and other leaf characteristics in the major tropical root crops, tannia, sweet potato, yam, cassava and taro. *Exp. Agric.* **2000**, *36*, 509–516. [CrossRef]
39. Ali, A.M. Using Hand-Held Chlorophyll Meters and Canopy Reflectance Sensors for Fertilizer Nitrogen Management in Cereals in Small Farms in Developing Countries. *Sensors* **2020**, *20*, 1127. [CrossRef]